

# Nonsynonymous C1653T Mutation of Hepatitis B Virus X Gene Enhances Malignancy of Hepatocellular Carcinoma Cells

Cuifang Zhang<sup>1,2</sup>, Ying Xie<sup>3</sup>, Ruixue Lai<sup>1</sup>, Jianhua Wu<sup>4</sup>, Zhanjun Guo<sup>1</sup>

<sup>1</sup>Department of Rheumatology and Immunology, The Fourth Hospital of Hebei Medical University, Shijiazhuang, People's Republic of China;

<sup>2</sup>Department of Oncology, The Pingshan County People's Hospital, Shijiazhuang, People's Republic of China; <sup>3</sup>Hebei Key Laboratory of Laboratory Animal Science, Hebei Medical University, Shijiazhuang, People's Republic of China; <sup>4</sup>Animal Center, The Fourth Hospital of Hebei Medical University, Shijiazhuang, People's Republic of China

Correspondence: Zhanjun Guo, Department of Rheumatology and Immunology, The Fourth Hospital of Hebei Medical University, 12 Jianshang Road, Shijiazhuang, 050011, People's Republic of China, Tel + 86 311 8609 5734, Fax + 86 311 8609 5237, Email zjguo5886@aliyun.com

**Purpose:** Functional analysis was performed to elucidate the mechanism by which hepatocellular carcinoma (HCC) outcome-associated mutation in the hepatitis B virus X (*HBx*) gene modifies the HCC process.

**Methods:** Proliferation, invasion, migration, and apoptosis assays were performed, and changes in fibrosis, intracellular reactive oxygen species (ROS), and cytokine levels were measured. The differences between variables were evaluated by Student's *t*-test.

**Results:** The influence of two previously identified nonsynonymous mutation, C1653T and T1753C, on HCC cells was assessed. With regard to HBX-induced promotion of proliferation ( $p < 0.01$ ), invasion ( $p < 0.01$ ) and migration ( $p < 0.01$ ), the C1653T mutation displayed a significant additive effect in these assays ( $P < 0.05$ ). The subsequent apoptosis assay indicated that HBX could inhibit apoptosis ( $P < 0.01$ ), whereas the C1653T mutation markedly amplified this effect in HCC cells ( $P < 0.01$ ). Furthermore, the tumor growth-promoting effect of HBX was confirmed in a mouse xenograft model of HCC ( $P < 0.05$ ), and the C1653T mutation was observed to amplify this effect ( $P < 0.05$ ). To further investigate the mechanism by which the C1653T mutation enhances malignancy in HCC cells, fibrosis, intracellular ROS, and cytokine levels were measured. The C1653T mutant increased fibrosis and intracellular ROS level, and altered monocyte chemoattractant protein-1 and interleukin-18 expression in HepG2 cells. Drug sensitivity test revealed that the C1653T mutation is sensitive to apatinib treatment and that overexpression of vascular endothelial growth factor might be involved in this process.

**Conclusion:** Our data indicate that the C1653T mutation of *HBx* promotes HCC malignancy by altering the levels of fibrosis, ROS, and some cytokines. This mutation could serve as a potential biomarker for screening HCC patients to determine apatinib treatment efficacy.

**Keywords:** HCC, HBV, HBX, C1653T mutation, apatinib, VEGF

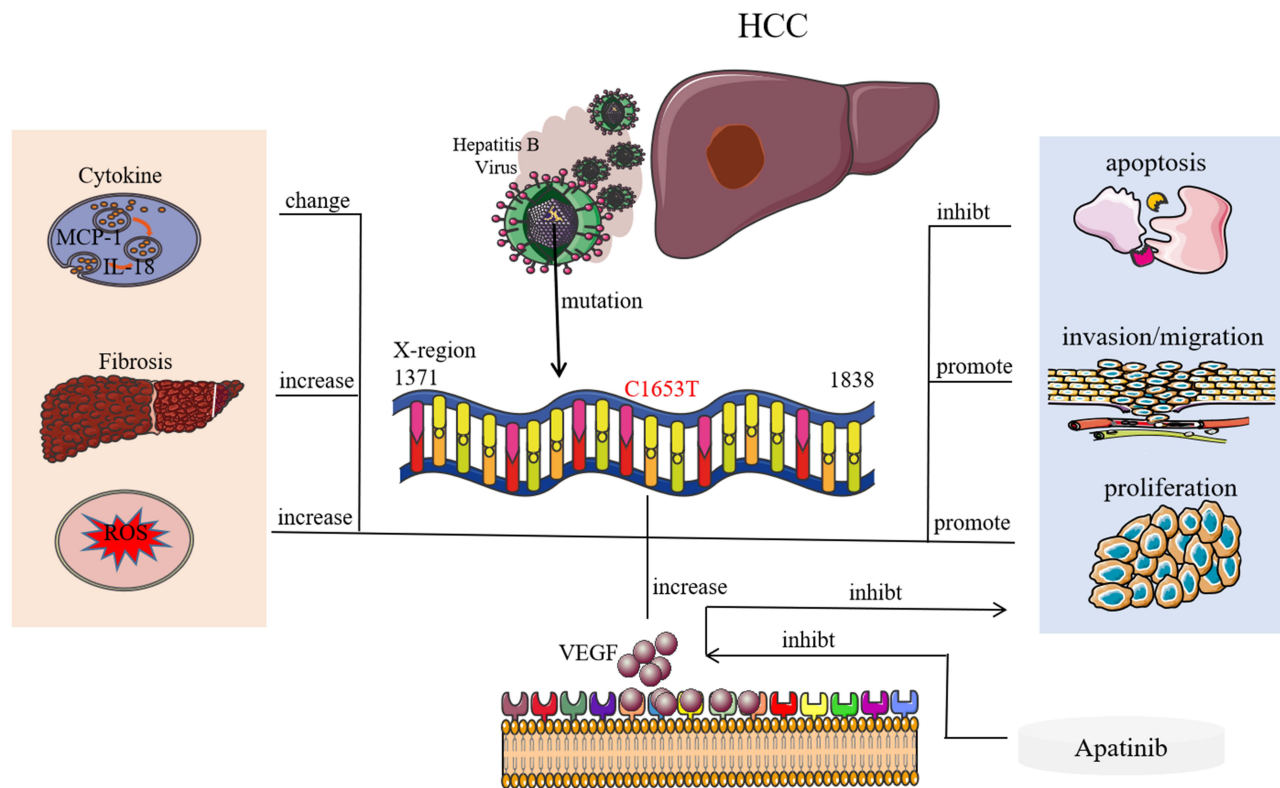
## Plain Language Summary

Two of *HBx* nonsynonymous mutations of the C1653T (94 Tyr-His) and T1753C (127 Ile-Thr) mutations which associated with HCC outcome were used to perform functional analysis. On the basis of HBX induced malignancy of HCC cells, the C1653T mutant could enhance this effect by changing the levels of fibrosis, ROS and some cytokines. Meanwhile, the C1653T mutation could be a potential biomarker for HCC patients screening with Apatinib treatment.

## Introduction

Hepatocellular carcinoma (HCC) was the third leading cause of cancer-related deaths worldwide in 2020, with 906,000 new cases and 830,000 deaths annually.<sup>1</sup> In China, HCC ranks fourth among all the cancers in terms of incidence.<sup>2</sup> The main risk factors for HCC are genetic predisposition, metabolic syndrome, alcohol consumption, exposure to aflatoxin B1, and chronic viral infection (hepatitis B and C viruses), with more than half of HCC cases worldwide related to hepatitis B virus (HBV) infection.<sup>3,4</sup> The incidence of HCC is higher in the Asia-Pacific and African regions than in other regions because of the high prevalence of HBV infection.<sup>5</sup>

## Graphical Abstract



HBV is a hepatotropic virus with four overlapping open reading frames encoding the surface protein, core protein, viral polymerase, and X protein (HBX), the proofreading deficiencies of HBV polymerase make its DNA prone to mutations.<sup>6</sup> HBX is a multifunctional nonstructural protein that regulates the activities of host cellular genes as a multifunctional oncoprotein for HCC.<sup>7,8</sup> It can drive cell oncogenesis by exerting effects on the cell cycle, cell growth and apoptosis, DNA repair, oxidative stress and epigenetic changes induced by miRNA.<sup>9,10</sup>

The *HBx* region contains critical cis-elements such as enhancer II, core promoter and miRNA-binding region with a length of 465 bp. *HBx* mutations with or without amino acid substitutions possibly modify HCC survival, including AG1762/1764TA (KV130/131MI), C1653T (H94Y), C1485T (P38S), T1753C (I127T), A1383C, and G1613A, but the functional analysis of these mutations remains unknown.<sup>11,12</sup> Our previous study also identified 12 mutations with 6 nonsynonymous mutations in the *HBx* region that could influence the outcome of HBV-related HCC (HBV-HCC).<sup>13</sup> C1653T (H94Y), one of the *HBx* nonsynonymous mutations located in the EnH II region, can alter the binding affinity of trans-regulated nuclear factors and induce His94Tyr amino acid substitution in the HBx protein, which contributes to worse outcomes in HCC.<sup>14</sup> In addition, another hepatocarcinogenesis-associated mutation, 1753C, could induce an I127A amino acid substitution, which affects HBx-induced apoptosis by changing the binding affinity of HBx to BCL2.<sup>15</sup> In the present study, the effects of the two *HBx* nonsynonymous mutations, C1653T (94 Tyr-His) and T1753C (127 Ile-Thr), on HCC cell malignance were evaluated by performing functional analysis.

## Materials and Methods

### Cell Culture and Transfection

HepG2 and Huh7 cell lines authenticated by short tandem repeat (STR) profiling were purchased from Shanghai Sangon Bioengineering Co., Ltd. (Shanghai, China) and Procell Life Science & Technology Co., Ltd. (Wuhan, Hubei, China),

respectively. All the cells were cultured in DMEM (Thermo Fisher, CA, USA) supplemented with 10% fetal bovine serum (FBS) (ZETA Life, CA, USA) in a humidified incubator containing 5% CO<sub>2</sub> at 37°C.

The full-length peptide coding sequence regions of *HBx*, *HBx* with C1653T mutation, and *HBx* with T1753C mutation were synthesized by Sangon and linked into pLVX-IRES-tdTomato (Clontech, Biovector Science Lab, Inc, Beijing, China) to package lentivirus. Stable clones were selected using 0.6 µg/mL puromycin, and successful transfections were confirmed by immunostaining and Western blotting for HBX.

## Immunostaining of HBX

All cell lines in the logarithmic growth phase were seeded into polylysine-coated six-well plates and immobilized with 4% paraformaldehyde. Cells were incubated with mouse monoclonal anti-HBX antibody (1:500; Santa Cruz, INC) for 5 h at 25°C after blocking with 5% skim milk and subsequently with secondary HRP-conjugated anti-mouse IgG antibody (1:10,000; Thermo Fisher, New York, NY) for 1 h at 25°C. HBX immunostaining was visualized directly using a microscope (Nikon, Tokyo, Japan, magnification, 200×).

## Western Blot Analysis

Total protein was extracted using radioimmunoprecipitation assay lysis buffer with freshly added protease inhibitor (Roche, Basel, Switzerland). Briefly, 60 µg of total protein was subjected to sodium dodecyl sulfate polyacrylamide gel electrophoresis and transferred onto a polyvinylidene difluoride membrane (Roche). The membranes were subsequently incubated with mouse monoclonal anti-HBX antibody (1:500; Santa Cruz) and rabbit monoclonal anti-vascular endothelial growth factor (VEGF) antibody (1:1000; HuaAn Biotechnology Co., Ltd., Hangzhou, China) overnight at 4°C after blocking with 5% skim milk for 2 h at 25°C. The sections were then incubated with secondary HRP-conjugated anti-mouse or anti-rabbit IgG antibodies (1:10,000; Thermo Fisher Scientific, New York, NY, USA). Proteins were visualized with WesternLumaxLight™ Peroxide (Zeta Life, USA) using the ChemiDoc™ Touch imaging system (Thermo Fisher, New York, NY, USA).

## Cell Proliferation Assay

Cell proliferation was measured using Cell Counting Kit-8 (CCK-8; Dojindo Lab, Kumamoto, Japan). Briefly, all cell lines in the logarithmic growth phase were seeded into 96-well microplates at a density of  $1 \times 10^3$  cells per well. At each time point (0, 24, 48, 72 and 96 h), 10 µL of diluted CCK-8 was added into each well, and cells were incubated in a 5% humidified CO<sub>2</sub> incubator for 2 h at 37°C. Absorbance at 450 nm was measured using a Microplate Autoreader (Bio-Tek; Instruments, Winooski, VT, USA).

## Cell Invasion and Migration Assays

Cell migration and invasion assays were performed using 8-µm transwell chambers containing polycarbonate filters (Corning, NY, USA) and precoated with Matrigel (BD Biosciences, NJ, USA), respectively. All cell lines in the logarithmic growth phase were disposed of with DMEM medium containing 2% FBS and placed in the upper chambers at a density of  $3 \times 10^4$  cells per well, and 600 µL DMEM medium containing 10% FBS was added to the lower chamber. After 48 h, cells that had invaded and migrated to the underside of the membrane were fixed with 4% methyl alcohol and stained with 0.1% crystal violet. The stained cells were counted under an inverted microscope in five randomly selected fields (magnification, 200×).

## Flow Cytometry for Apoptosis Assay

Apoptosis was assessed using flow cytometry. The harvested cells were washed twice with cold PBS and once with a binding buffer and incubated with PE-conjugated Annexin V and 7-AAD (BD Biosciences, Pharmingen, San Diego, CA, USA) for 15 min in the dark at 25°C. The cells were resuspended in a binding buffer and analyzed using a fluorescence-activated cell sorting Aria II flow cytometer (BD Biosciences). Each experiment was repeated thrice.

## Fibrosis Measurement

The fibrosis markers of hyaluronan (HA), aminoterminal propeptide of type III procollagen (PIII NP), and type IV collagen (Col IV) were measured by chemiluminescence immunoassay using HA, PIIINP, and Col IV detection kits (Mindray Biological Medical Co., Ltd., Shenzhen, China), respectively, according to the manufacturer's instructions. Data were measured using a CL-2200i automatic chemiluminescence immunoanalyzer (Mindray Biological Medical).

## Intracellular Reactive Oxygen Species (ROS) Measurement

All the cells in the logarithmic growth phase were seeded into 96-well plates at a density of  $1 \times 10^4$  cells/well for 48 h and incubated with 100  $\mu$ L dichloro-dihydro-fluorescein diacetate dye (Dojindo, Kyushu Island, Japan) in a 5% humidified CO<sub>2</sub> incubator for 30 min at 37°C. Fluorescence intensity was examined at 500 nm and 540 nm using a fluorescent microplate reader (Biotek Synergy, VT, USA).

## Cytokines Detection

Twelve cytokines, including (IFN)- $\alpha$ 2, IFN- $\gamma$ , tumor necrosis factor- $\alpha$  (TNF)- $\alpha$ , monocyte chemotactic protein-1 (MCP-1), interleukin (IL) -6, IL-18, IL-1 $\beta$ , IL-10, IL-12p70, IL-17A, IL-23 and IL-33 were tested in Hebei Senlangbio Biotechnology Co., Ltd. (Shijiazhuang, China) using a flow fluorescence immunomicrobead assay. Briefly,  $2 \times 10^5$  cells/well were seeded into six-well plates for 72 h, and 25  $\mu$ L culture medium was diluted 2-fold with the assay buffer and incubated with 25  $\mu$ L of microbeads and detection antibody at 25°C for 2 h in the dark. To each medium, 25  $\mu$ L streptavidin-phycoerythrin (SA-PE) was added followed by shaking at approximately 500 rpm for 30 min at 25°C in the dark. MACSQuant Analyzer 10 flow cytometer (Miltenyi Biotec, Bergisch Gladbach, Germany) was used to quantify the PE fluorescence signal of the analyte-specific bead region, and BioLegend's LEGENDplex™ Data Analysis Software (Biolegend, San Diego, CA) was used to generate a standard curve and determine the concentration of the specific analyte. The absolute concentrations in the serum were calculated using known standards.

## Drug Sensitivity Assay

Apatinib was purchased from Dalian Meilun Biotechnology Co. Ltd. (Dalian, China). HepG2 cell lines were seeded into six-well plates at a density of  $3 \times 10^4$  cells per well. Apatinib at varying concentrations (2.5, 5, and 10  $\mu$ mol/L) was added to each group and incubated for 72 h. Proliferation assay was subsequently performed to determine drug sensitivity.

## Mouse Xenograft Tumor Model

Twenty-four 4-week-old male BALB/cA nude mice were purchased from Beijing HFK Bioscience Co., Ltd. [Beijing, China; Permission No. SCXK (Jing) 2019-0008]. Nude mice were kept in a specific-pathogen-free environment of the Center of Laboratory Animal Research and Service of Hebei Medical University and treated in accordance with the National Institutes of Health Guide for the Care and Use of Laboratory Animals. This study was supervised and approved by the Ethics Board of the Animal Ethics Committee of the Hebei Medical University.

HepG2 cells ( $1 \times 10^7$  cells/mouse) stably transfected with wild-type (WT) HBx or HBx with C1653T mutations were subcutaneously injected into the right scapular region of each mouse. Tumor growth was monitored at regular intervals by measuring the tumor diameter using a caliper. Tumor volume was determined using the following formula: volume = length  $\times$  (width)<sup>2</sup>/2.

## Statistical Analysis

Data are expressed as mean  $\pm$  standard deviation. All comparisons were performed using unpaired Student's *t*-test. Statistical analysis was set up at  $P < 0.05$ . Statistical analysis was performed using SPSS software (version 21.0; SPSS Inc. Chicago, IL, USA).

## Results

### C1653T Mutant Enhanced HCC Cell Malignancy

The successful transfection of HepG2 and Huh7 cell lines with WT *HBx* (HBX group), *HBx* with C1653T mutation (1653 group), and *HBx* with T1753C mutation (1753 group) was confirmed by immunostaining and Western blotting. The HepG2 and Huh7 cell lines were used as blank controls (Figure 1).

CCK-8 assay revealed that both HepG2 and Huh7 cells transfected with HBX and mutated proteins displayed increased proliferation capacity compared to blank control ( $p < 0.01$ ) from 24 to 96 h after incubation (Figures 2A and S1A). With regard to HBX-induced proliferation, 1653 group displayed a further additive effect on proliferation from 24 to 96 h ( $p < 0.05$ ) compared to the HBX group, 1753 group showed almost the same trend as the HBX group (Figures 2A and S1A).

Transwell assays were performed to measure the invasion and migration capacities of HCC cells. Both C1653T and HBX promoted the invasion ( $p < 0.01$ ) and migration ( $p < 0.01$ ) capacity of HepG2 and Huh7 cells compared to blank

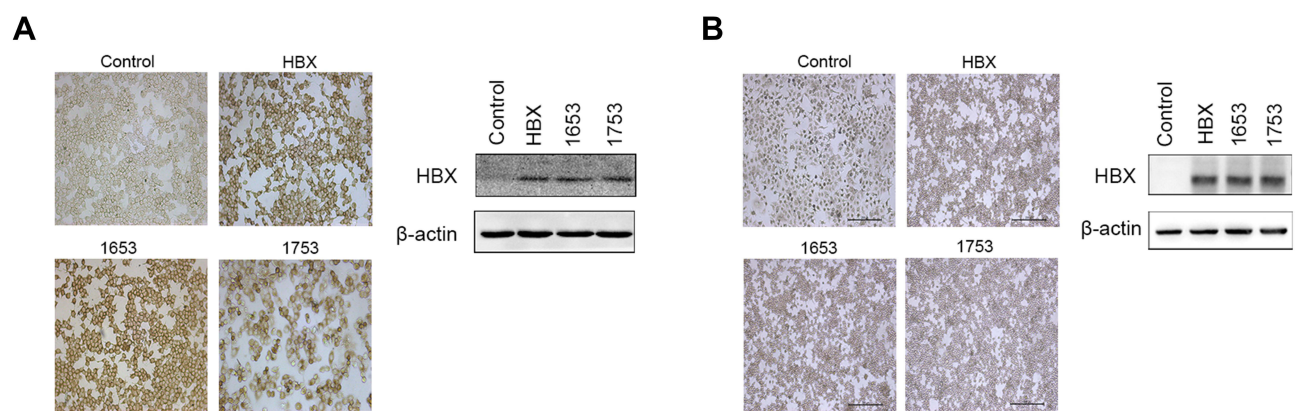


**Figure 1** Expression of HBX in the four groups. (A) Immunostaining and Western blot analysis of HBX for Control, HBX, 1653 and 1753 groups in HepG2 cells. (B) Immunostaining and Western blotting analysis of HBX for Control, HBX, 1653 and 1753 groups in Huh7 cells.

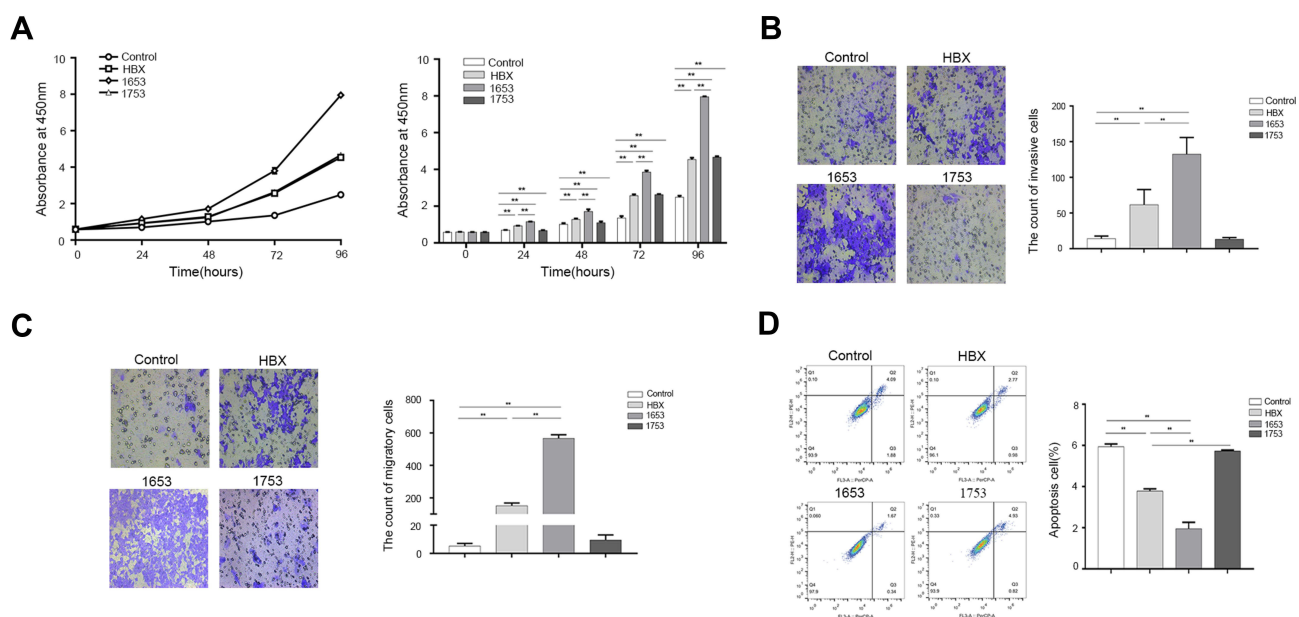


**Figure 2** The functional analysis indicated that C1653T mutation enhanced the malignancy of HepG2 cells. (A) CCK-8 assay for Control, HBX, 1653 and 1753 groups. (B) Cell invasion assay for Control, HBX, 1653 and 1753 groups. (C) Cell migration assay for Control, HBX, 1653 and 1753 groups. (D) Flow cytometry assay for Control, HBX, 1653 and 1753 groups. \*\* $P < 0.01$ .

control; C1653T also amplified HBX-induced invasion ( $p < 0.01$ ) and migration ( $p < 0.01$ ), whereas the T1753C did not increase cell invasion and migration compared to blank control (Figures 2B and C, S1B and C).

Apoptosis analysis by flow cytometry showed that, compared with blank control, HBX decreased the apoptosis rate of HepG2 and Huh7 cells, whereas C1653T significantly amplified this effect ( $p < 0.01$ ). In addition, no difference was observed between the 1753 and blank control groups in terms of the apoptosis rate (Figures 2D and S1D).

The aforementioned data indicate that HBX promotes HCC cell malignancy by promoting proliferation, invasion, migration and apoptosis; the C1653T mutant amplifies this malignancy.

To further evaluate the effect of the C1653T mutation on tumor growth in vivo, the growth rates of the HepG2 cell-derived xenograft model of HBX and 1653 groups were compared to that of the blank control. The growth of the HBX group xenografts was significantly increased compared with that of the blank control ( $p < 0.05$ ), and C1653T displayed further additive effects for xenografts at 15 days after implantation ( $p < 0.05$ ) according to caliper measurements. These results suggest that the C1653T mutant promotes HBX-induced growth of HCC cells in vivo (Figure 3).

## C1653T Mutant Increased Fibrosis and ROS Level and Altered Cytokines Level of HCC Cells

To evaluate the mechanism of C1653T mutation-related malignancy in HCC cells, we assessed changes in the fibrosis levels of HepG2 cells in the C1653T mutant. The fibrosis indices of HA, PIII NP and Col IV were measured. HA level was increased upon HBx transfection ( $p < 0.01$ ). In addition to amplifying HBx-related increase in HA levels ( $p < 0.01$ ), the C1653T mutant also increase Col IV levels ( $p < 0.01$ ) compared with the blank control and HBX groups. The T1753C mutation only increased HA levels ( $p < 0.01$ ) compared with the blank control (Figure 4A). The PIII NP levels of these groups were not significantly different (data not shown).

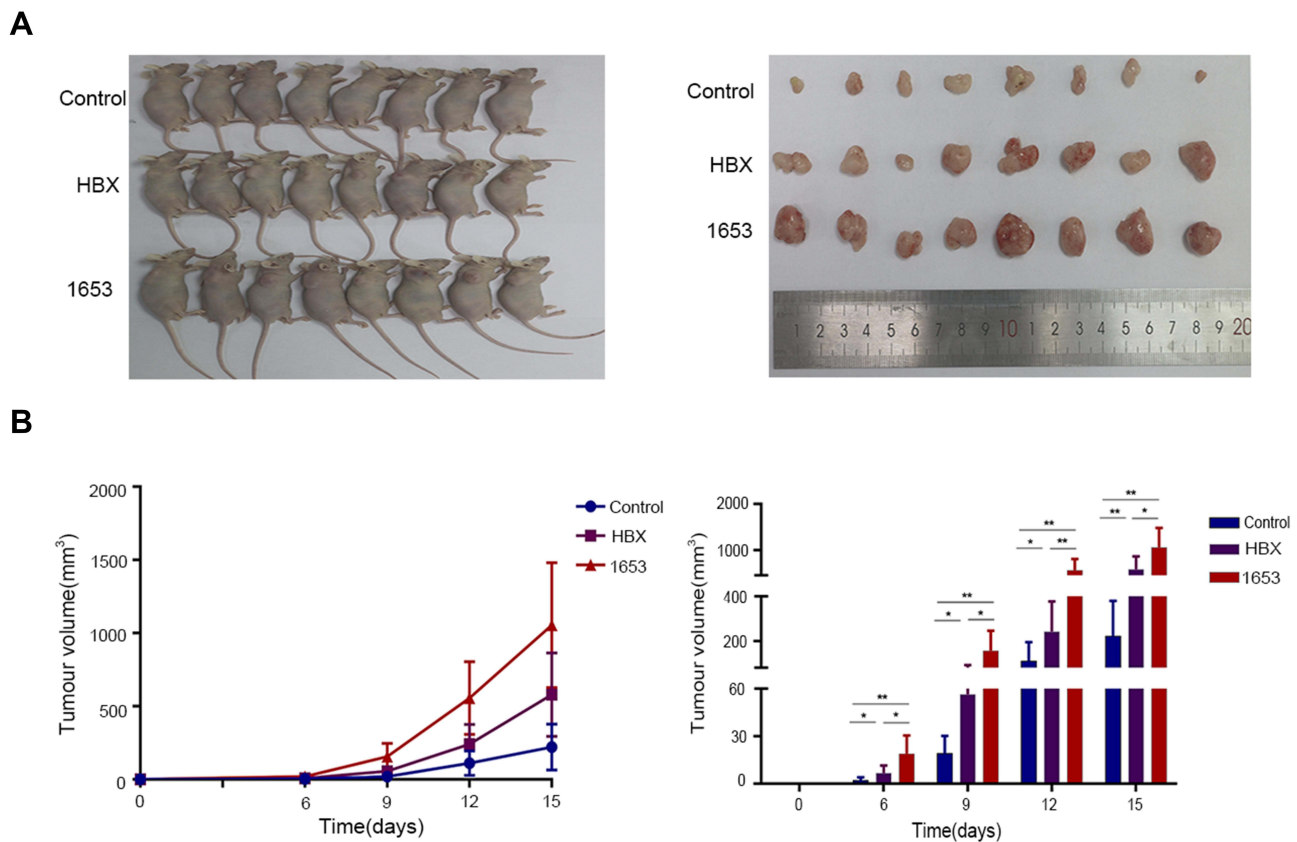


**Figure 3** Mouse xenograft tumor model indicated that C1653T mutant enhanced growth of HepG2 cells in vivo. (A) Tumor growth was monitored by measuring tumor volume for HepG2 xenografts ( $n = 8$  for each group). (B) Growth curves of xenograft tumours. \*\* $P < 0.01$ , \* $P < 0.05$ .

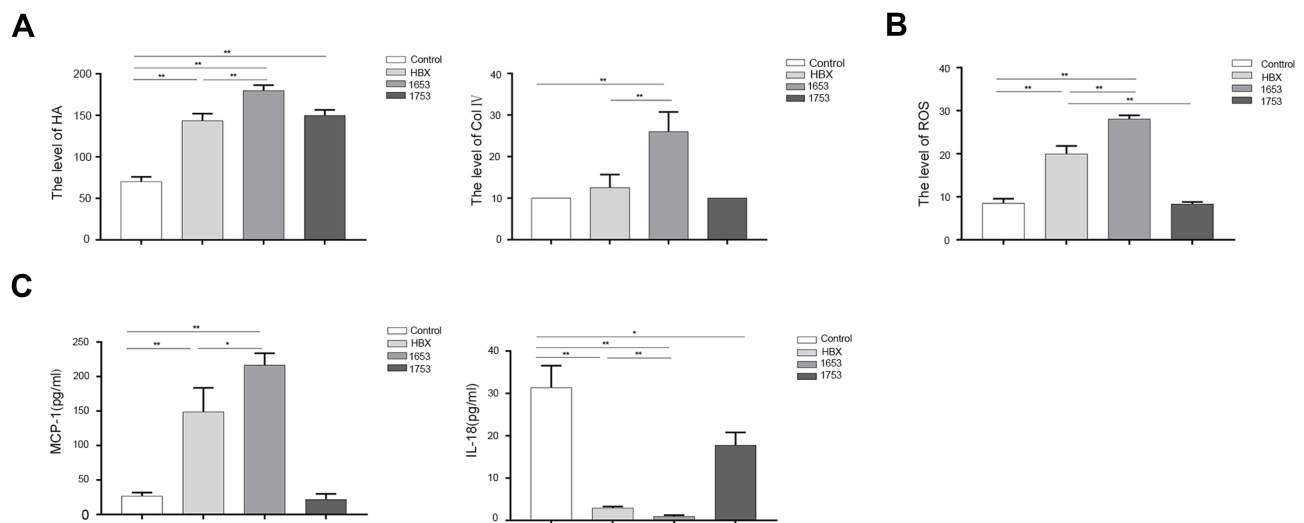


**Figure 4** Measurement of fibrosis, ROS and cytokines levels. **(A)** Fibrosis levels of HA and Col IV in Control, HBX, 1653 and 1753 groups. **(B)** ROS levels in Control, HBX, 1653 and 1753 groups. **(C)** Cytokines levels of MCP-1 and IL-18 in Control, HBX, 1653 and 1753 groups. \*\* $P < 0.01$ , \* $P < 0.05$ .

Comparison of the ROS levels of the four groups revealed that ROS levels of the 1653 and HBX groups were significantly higher than those of the blank control ( $p < 0.01$ ). The C1653T mutant generated more ROS than the HBX group ( $p < 0.01$ ), whereas the T1753C mutant had no influence on ROS generation (Figure 4B). These data imply that the C1653T mutant enhances malignancy of HCC cells malignancy by increasing fibrosis and ROS levels; however, not all HBV mutations exhibit malignant effects on HCC development.

Since HBX could alter the levels of some cytokines, such as IL-6, IL-18 and MCP-1,<sup>16,17</sup> the level of cytokines IFN- $\alpha 2$ , INF- $\gamma$ , TNF- $\alpha$ , MCP-1, IL-18, IL-1 $\beta$ , IL-6, IL-10, IL-12p70, IL-17A, IL-23 and IL-33 were assessed among these groups in HepG2 cells among these groups (Figure S2). The levels of the two cytokines, MCP-1 and IL-18, were found to be significantly different among these groups. The HBX and 1653 groups showed increased MCP-1 but decreased IL-18 levels compared to the blank control group ( $p < 0.01$ ), and an additive effect of C1653T mutation on HBX-induced cytokine changes was also observed when comparing these two groups ( $p < 0.05$ ) (Figure 4C). The T1753C mutation also decreased IL-18 levels (T1753C vs control,  $p < 0.05$ ) but to a lesser degree compared to WT HBX and C1653T mutation (T1753C vs 1653,  $p < 0.01$ ; T1753C vs WT,  $p < 0.01$ ) (Figure 4C).

## C1653T Mutant Was Sensitive to Apatinib Treatment

Apatinib is used in China as a second-line treatment for HCC, and we checked the treatment efficiency of apatinib on HepG2 cells with HBX mutations. After screening for the optimal concentration of apatinib (Figure 5A), the concentrations of 2.5 and 5  $\mu\text{mol/L}$  were used for the drug sensitivity test. The growth of cells in the blank control, HBX, and 1653 groups were inhibited by apatinib at 48 to 72 h in the proliferation assay; however, the 1753 group cells were resistant to apatinib treatment (Figure 5B and C). The apatinib-induced inhibition was time dependent. At 72 h, the growth inhibition rates of HCC cells in the blank control, HBX, and 1653 treated with 2.5  $\mu\text{mol/L}$  apatinib were 19.2%, 20% and 23.7%, respectively, whereas those treated with 5  $\mu\text{mol/L}$  apatinib were 26.3%, 23.8% and 69.7%, respectively (Figure 5B and C). These data indicate that the C1653T mutant was sensitive to apatinib treatment although it enhanced HCC cells malignancy. VEGF level of the apatinib-targeting pathway displayed a gradual increase from the control to the HBX and 1653 groups (Figure 5D). These data indicate that C1653T mutation is sensitive to apatinib treatment and that overexpressed VEGF might involve in this process.

## Discussion

HBX modulates cytoplasmic signal transduction pathways, including focal adhesion kinase, proline-rich tyrosine kinase 2, protein kinase C and Src-dependent phosphatidylinositol-3 kinase (PI3K/Akt), to activate HBV DNA replication and

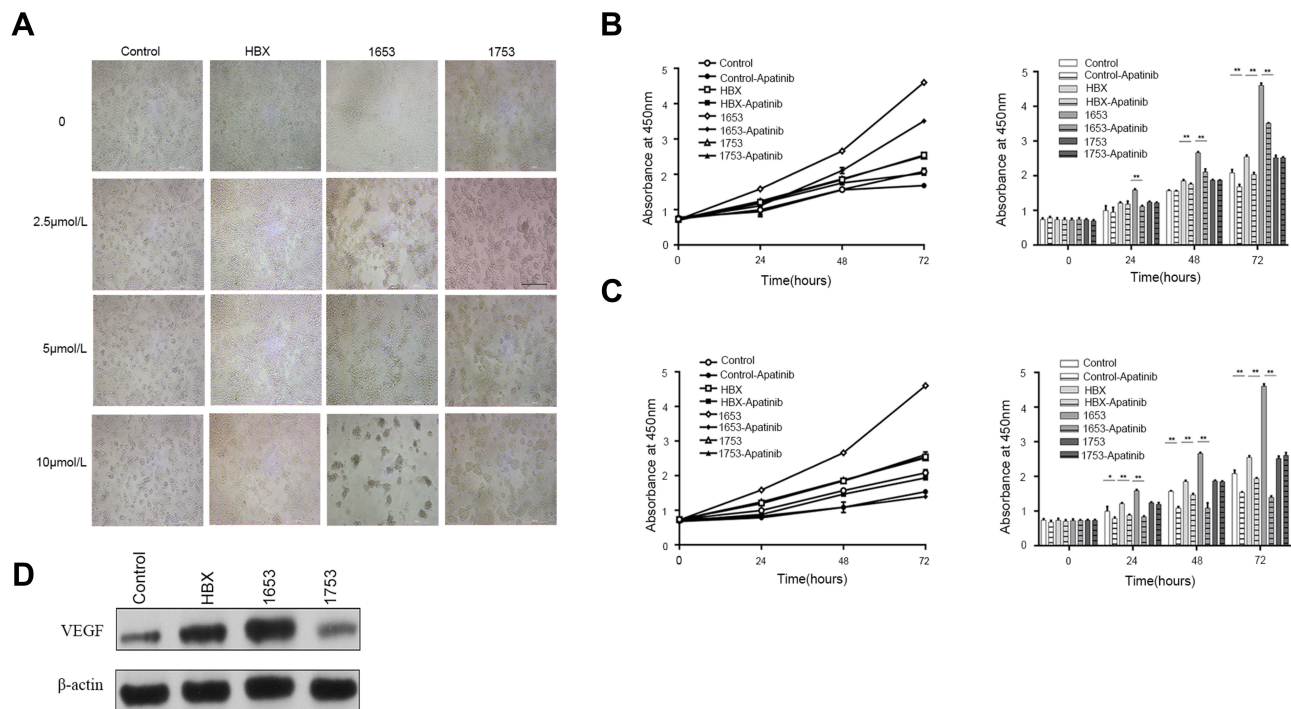


**Figure 5** Drug sensitivity test for apatinib. **(A)** Apatinib concentration screening showed that 2.5 and 5 μmol/L apatinib was suitable for subsequent proliferation assay. **(B)** 2.5 μmol/L apatinib proliferation assay for Control, HBX, 1653 and 1753 groups. **(C)** 5 μmol/L apatinib proliferation assay for Control, HBX, 1653 and 1753 groups. **(D)** Western blotting analysis of VEGF expression. \*\* $P < 0.01$ , \* $P < 0.05$ .

hepatic cell proliferation.<sup>18–20</sup> It also interacts with p53 or cortactin (*CTTN*) to promote the HCC cell proliferation and migration.<sup>21,22</sup> Therefore, *HBx* mutations might modify the clinical course of chronic HBV infection and hepatocarcinogenesis by altering the functions of *HBx*.

Previous studies reported that mutations C1653T and T1753C in *HBx* were associated with the risk of HCC, and our previous studies identified that these two mutations could influence the outcome of HCC; however, functional analysis for these mutations has not been performed yet.<sup>7,13</sup> The results of our functional analysis of proliferation, invasion, migration, and apoptosis of these two mutations suggest that the C1653T mutant enhances *HBx*-induced malignancy in HCC cells. The impact of *HBx* on the regulation of apoptotic pathways is contradictory; some studies have shown that *HBx* inhibits cellular apoptosis,<sup>23–25</sup> whereas other studies have reported that *HBx* enhances cell death.<sup>26</sup> Such contradictory manifestations depended on the differential pattern of *HBx* expression and the cell type involved. *HBx* directly inhibits apoptosis by upregulating the nuclear factor  $\kappa$ B (NF- $\kappa$ B) and PI3K pathways in HepG2 cells.<sup>27,28</sup> The subsequent analysis implied that changes in fibrosis and the level of intracellular ROS and some cytokines might be responsible for this enhanced malignancy in the presence of C1653T mutation. The final drug test revealed that this mutation is sensitive to apatinib treatment and that VEGF overexpression might be involved in this process. However, based on our analysis, the T1753C mutant did not enhance the malignancy of HCC cells. The HCC outcome-associated HBV mutations identified by clinical analysis should be validated by functional analysis, at least at the cellular level. The C1653T mutation could change the binding affinity between the HBV promoter and HBV replication factor of the CCAAT/enhancer binding protein, thereby modifying HBV replication.<sup>29</sup> However, functional change induced in the *HBx* protein due to the C1653T mutation that results in a histidine to tyrosine substitution at codon 94 needs further investigation.

Most newly diagnosed HCC patients are at a late stage with advanced fibrosis or cirrhosis, which are the major risk factors for HCC. Liver fibrosis alters HCC development by modulating changes in tumor microenvironment including tumor angiogenesis, extracellular matrix, immune surveillance and cytokines secretion, thereby promoting tumor cell proliferation, migration, and invasion through with direct and indirect pathways.<sup>30,31</sup> We found that *HBx* and the C1653T mutant increased the fibrosis level of HCC cells, which might explain the C1653T mutation enhanced



malignancy in HCC cells. ROS are generated as by-products of oxygen consumption and cellular metabolism that induce DNA damage, protein denaturation and lipid peroxidation to initiate HCC.<sup>32,33</sup> They activate the transcription factors STAT-3 and NF- $\kappa$ B to stimulate the mitochondrial translocation of Raf-1, thereby accelerating HCC progression.<sup>34</sup> ROS also trigger TRPA1-mediated Ca<sup>2+</sup> influx into cells to activate potassium channels thereby increasing HCC cell proliferation and migration.<sup>35–38</sup> Moreover, ROS can facilitate epithelial–mesenchymal transition (EMT) and metastasis in HCC via Nrf2/Notch signaling pathway.<sup>39</sup> HBX can increase ROS production by downregulating quinone oxidoreductase 1, a mitochondrial enzyme related to electron transport and intracellular glutathione levels.<sup>40</sup> ROS can initiate hepatic fibrosis by activating hepatic stellate cells and NF- $\kappa$ B.<sup>41</sup> It is possible that increasing fibrosis and ROS levels and/or their interaction mediates the C1653T mutation enhanced malignancy of HCC cells. E-cadherin and N-cadherin expression levels were also measured to check whether the C1653T mutant promote EMT, thereby enhancing HCC cell malignancy, but negative results were obtained (data not shown).

Cytokines are secreted by various cells that act as vital regulators in many physiological processes including tumor progression and immune response.<sup>42</sup> MCP-1 is a member of the CC chemokine family that recruits the migration and infiltration of monocytes/macrophages or increases tumor vascularity to facilitate tumor progression and metastasis, thus, higher MCP-1 levels correlate with a reduced lifespan in cancer patients, including HCC patients.<sup>43,44</sup> The induction of miR-21 by MCP-1 can initiate EMT in HCC cells to promote the HCC intrahepatic metastasis.<sup>45</sup> MCP-1 mediated tumor vascular formation promotes the HCC metastasis via the FGFR3 signaling pathway.<sup>46</sup> The excessive production of ROS triggers the release of MCP-1 by inhibiting the phosphorylation of p38 and activating of the I $\kappa$ B $\alpha$ /NF- $\kappa$ B pathway.<sup>17</sup> The C1653T mutant-induced MCP-1 overexpression might contribute to the enhanced malignancy observed in these cells through the aforementioned mechanism. IL-18 is a member of the IL-1 family and is associated with hepatic fibrosis.<sup>47</sup> It exerts inflammation-dependent tumor-suppressive effects by promoting the differentiation, activity and survival of tumor-infiltrating T cells.<sup>48,49</sup> In summary, the final effect of the C1653T mutant-related cytokine changes on HCC growth was at least partly determined by these two cytokines and their interaction with fibrosis.

Apatinib is a new tyrosine kinase inhibitor that exhibits significant antitumor activity in several solid tumors including HCC and gastric cancer by targeting VEGF receptor-2 (VEGFR-2) to inhibit tumor angiogenesis.<sup>50,51</sup> Fibrosis promotes angiogenesis by upregulating the expression of VEGF and its receptor VEGFR-2;<sup>30</sup> high ROS also increases the secretion of VEGF.<sup>52</sup> Autocrine VEGF-induced VEGFR2 overexpression can enhance the treatment efficiency of apatinib in gastric cancer.<sup>53</sup> We found that VEGF was highly expressed in the C1653T mutant; hence, the C1653T mutant-induced VEGF overexpression through ROS and the fibrosis pathway might provide more targets for apatinib with elevated VEGF levels, which would partly explain the sensitivity of the C1653T mutant to apatinib treatment. Another VEGF inhibitor, sorafenib, a multi-target tyrosine kinase inhibitor applied in HCC treatment, needs to be tested for its sensitivity against the C1653T mutant HCC in further studies.

In conclusion, our data indicate that the C1653T mutation of *HBx* promotes HCC malignancy by altering the levels of fibrosis, ROS and some cytokines. This mutation could serve as a potential biomarker for screening HCC patients to determine apatinib treatment efficacy.

## Ethics Approval and Consent to Participate

This article does not include any studies with human participants or animals performed by any of the authors.

## Data Sharing Statement

All data generated or analyzed during this study are included in this published article (more information, please contact the corresponding author).

## Funding

This work was supported by the Natural Science Foundation of China of Hebei Province (Grant No. H2019206428) and the Foundation of Hebei Provincial Department of Science and Technology & Hebei Medical University, Shijiazhuang, Hebei (Grant No. 2020TXZH03).

## Disclosure

The authors declare that they have no competing interests.

## References

- Sung H, Ferlay J, Siegel RL, et al. Global cancer statistics 2020: GLOBOCAN estimates of incidence and mortality worldwide for 36 cancers in 185 countries. *CA Cancer J Clin.* 2021;71(3):209–249. PubMed:33538338. doi:10.3322/caac.21660
- Li B, Yan C, Zhu J, et al. Anti-PD-1/PD-L1 blockade immunotherapy employed in treating hepatitis B virus infection-related advanced hepatocellular carcinoma: a literature review. *Front Immunol.* 2020;11:1037. PubMed:32547550.
- European Association For The Study Of The Liver. EASL-EORTC clinical practice guidelines: management of hepatocellular carcinoma. *J Hepatol.* 2012;56(4):908–943. PubMed:22424438. doi:10.1016/j.jhep.2011.12.001
- Yang JD, Hainaut P, Gores GJ, et al. A global view of hepatocellular carcinoma: trends, risk, prevention and management. *Nat Rev Gastroenterol Hepatol.* 2019;16(10):589–604. PubMed:31439937. doi:10.1038/s41575-019-0186-y
- Torre LA, Bray F, Siegel RL, et al. Global cancer statistics, 2012. *CA Cancer J Clin.* 2015;65(2):87–108. PubMed:25651787. doi:10.3322/caac.21262
- Yang HI, Yeh SH, Chen PJ, et al. Associations between hepatitis B virus genotype and mutants and the risk of hepatocellular carcinoma. *J Natl Cancer Inst.* 2008;100(16):1134–1143. PubMed:18695135. doi:10.1093/jnci/djn243
- Shinkai N, Tanaka Y, Ito K, et al. Influence of hepatitis B virus X and core promoter mutations on hepatocellular carcinoma among patients infected with subgenotype C2. *J Clin Microbiol.* 2007;45(10):3191–3197. PubMed:17652471. doi:10.1128/JCM.00411-07
- Murakami S. Hepatitis B virus X protein: a multifunctional viral regulator. *J Gastroenterol.* 2001;36(10):651–660. PubMed:11686474. doi:10.1007/s005350170027
- Muroyama R, Kato N, Yoshida H, et al. Nucleotide change of codon 38 in the X gene of hepatitis B virus genotype C is associated with an increased risk of hepatocellular carcinoma. *J Hepatol.* 2006;45(6):805–812. PubMed:17050029. doi:10.1016/j.jhep.2006.07.025
- Kim YJ, Jung JK, Lee SY, et al. Hepatitis B virus X protein overcomes stress-induced premature senescence by repressing p16(INK4a) expression via DNA methylation. *Cancer Lett.* 2010;288(2):226–235. PubMed:19656618. doi:10.1016/j.canlet.2009.07.007
- Guo X, Jin Y, Qian G, et al. Sequential accumulation of the mutations in core promoter of hepatitis B virus is associated with the development of hepatocellular carcinoma in Qidong, China. *J Hepatol.* 2008;49(5):718–725. PubMed:18801591. doi:10.1016/j.jhep.2008.06.026
- Kumar V, Jayasuryan N, Kumar R. A truncated mutant (residues 58–140) of the hepatitis B virus X protein retains transactivation function. *Proc Natl Acad Sci U S A.* 1996;93(11):5647–5652. PubMed:8643631. doi:10.1073/pnas.93.11.5647
- Xie Y, Liu S, Zhao Y, et al. X protein mutations in hepatitis B virus DNA predict postoperative survival in hepatocellular carcinoma. *Tumour Biol.* 2014;35(10):10325–10331. PubMed:25034530. doi:10.1007/s13277-014-2331-0
- Li SK, Ho SF, Tsui KW, et al. Identification of functionally important amino acid residues in the mitochondria targeting sequence of hepatitis B virus X protein. *Virology.* 2008;381(1):81–88. PubMed:18805561. doi:10.1016/j.virol.2008.07.037
- Geng X, Harry BL, Zhou Q, et al. Hepatitis B virus X protein targets the Bcl-2 protein CED-9 to induce intracellular Ca<sup>2+</sup> increase and cell death in *Caenorhabditis elegans*. *Proc Natl Acad Sci USA.* 2012;109(45):18465–18470. PubMed:23091037. doi:10.1073/pnas.1204652109
- Lee MO, Choi YH, Shin EC, et al. Hepatitis B virus X protein induced expression of interleukin 18 (IL-18): a potential mechanism for liver injury caused by hepatitis B virus (HBV) infection. *J Hepatol.* 2002;37(3):380–386. PubMed:12175634. doi:10.1016/S0168-8278(02)00181-2
- He T, Zhang N, Wang L, et al. GPR43 regulates HBV X protein (HBx)-induced inflammatory response in human LO(2) hepatocytes. *Biomed Pharmacother.* 2020;123:109737. PubMed:31884344. doi:10.1016/j.biopha.2019.109737
- Rawat S, Bouchard MJ. The hepatitis B virus (HBV) HBx protein activates AKT to simultaneously regulate HBV replication and hepatocyte survival. *J Virol.* 2015;89(2):999–1012. PubMed:25355887. doi:10.1128/JVI.02440-14
- Bouchard MJ, Wang LH, Schneider RJ. Calcium signaling by HBx protein in hepatitis B virus DNA replication. *Science.* 2001;294(5550):2376–2378. PubMed:11743208. doi:10.1126/science.294.5550.2376
- Zhu M, Li W, Lu Y, et al. HBx drives alpha fetoprotein expression to promote initiation of liver cancer stem cells through activating PI3K/AKT signal pathway. *Int J Cancer.* 2017;140(6):1346–1355. PubMed:27925189. doi:10.1002/ijc.30553
- Park SG, Min JY, Chung C, et al. Tumor suppressor protein p53 induces degradation of the oncogenic protein HBx. *Cancer Lett.* 2009;282(2):229–237. PubMed:19375220. doi:10.1016/j.canlet.2009.03.019
- Li Y, Fu Y, Hu X, et al. The HBx-CTTN interaction promotes cell proliferation and migration of hepatocellular carcinoma via CREB1. *Cell Death Dis.* 2019;10(6):405. PubMed:31138777. doi:10.1038/s41419-019-1650-x
- Shi Y, Wang J, Wang Y, et al. A novel mutant 10Ala/Arg together with mutant 144Ser/Arg of hepatitis B virus X protein involved in hepatitis B virus-related hepatocarcinogenesis in HepG2 cell lines. *Cancer Lett.* 2016;371(2):285–291. PubMed:26706415. doi:10.1016/j.canlet.2015.12.008
- Yun C, Um HR, Jin YH, et al. NF-kappaB activation by hepatitis B virus X (HBx) protein shifts the cellular fate toward survival. *Cancer Lett.* 2002;184(1):97–104. PubMed:12104053. doi:10.1016/S0304-3835(02)00187-8
- Wu G, Yu F, Xiao Z, et al. Hepatitis B virus X protein downregulates expression of the miR-16 family in malignant hepatocytes in vitro. *Br J Cancer.* 2011;105(1):146–153. PubMed:21629246. doi:10.1038/bjc.2011.190
- Terradillos O, Pollicino T, Lecoecur H, et al. p53-independent apoptotic effects of the hepatitis B virus HBx protein in vivo and in vitro. *Oncogene.* 1998;17(16):2115–2123. PubMed:9798683. doi:10.1038/sj.onc.1202432
- Shih WL, Kuo ML, Chuang SE, et al. Hepatitis B virus X protein inhibits transforming growth factor-beta -induced apoptosis through the activation of phosphatidylinositol 3-kinase pathway. *J Biol Chem.* 2000;275(33):25858–25864. PubMed:10835427. doi:10.1074/jbc.M003578200
- Liu Y, Lou G, Wu W, et al. Involvement of the NF-kB pathway in multidrug resistance induced by HBx in a hepatoma cell line. *J Viral Hepat.* 2011;18(10):e439–e446. PubMed:21914061. doi:10.1111/j.1365-2893.2011.01463.x
- López-Cabrera M, Letovsky J, Hu KQ, et al. Multiple liver-specific factors bind to the hepatitis B virus core/pregenomic promoter: trans-activation and repression by CCAAT/enhancer binding protein. *Proc Natl Acad Sci USA.* 1990;87(13):5069–5073. PubMed:2367525. doi:10.1073/pnas.87.13.5069

30. Baglieri J, Brenner DA, Kisseleva T. The role of fibrosis and liver-associated fibroblasts in the pathogenesis of hepatocellular carcinoma. *Int J Mol Sci.* 2019;20(7):1723. PubMed:30959975. doi:10.3390/ijms20071723
31. Hernandez-Gea V, Toffanin S, Friedman SL, et al. Role of the microenvironment in the pathogenesis and treatment of hepatocellular carcinoma. *Gastroenterology.* 2013;144(3):512–527. PubMed:23313965. doi:10.1053/j.gastro.2013.01.002
32. Moloney JN, Cotter TG. ROS signalling in the biology of cancer. *Semin Cell Dev Biol.* 2018;80:50–64. PubMed:28587975. doi:10.1016/j.semcdb.2017.05.023
33. Yu F, Wei J, Cui X, et al. Post-translational modification of RNA m6A demethylase ALKBH5 regulates ROS-induced DNA damage response. *Nucleic Acids Res.* 2021;49(10):5779–5797. PubMed:34048572. doi:10.1093/nar/gkab415
34. Peerzada KJ, Faridi AH, Sharma L, et al. Acteoside mediates chemoprevention of experimental liver carcinogenesis through STAT-3 regulated oxidative stress and apoptosis. *Environ Toxicol.* 2016;31(7):782–798. PubMed:26990576. doi:10.1002/tox.22089
35. Takahashi N, Chen HY, Harris IS, et al. Cancer cells co-opt the neuronal redox-sensing channel TRPA1 to promote oxidative-stress tolerance. *Cancer Cell.* 2018;33(6):985–1003. PubMed:29805077. doi:10.1016/j.ccell.2018.05.001
36. Déliot N, Constantin B, Constantin B. Plasma membrane calcium channels in cancer: alterations and consequences for cell proliferation and migration. *Biochim Biophys Acta.* 2015;1848(10 Pt B):2512–2522. PubMed:26072287. doi:10.1016/j.bbamem.2015.06.009
37. He Y, Lin Y, He F, et al. Role for calcium-activated potassium channels (BK) in migration control of human hepatocellular carcinoma cells. *J Cell Mol Med.* 2021;25(20):9685–9696. PubMed:34514691. doi:10.1111/jcmm.16918
38. Yang XW, Liu JW, Zhang RC, et al. Inhibitory effects of blockage of intermediate conductance Ca(2+)-activated K (+) channels on proliferation of hepatocellular carcinoma cells. *J Huazhong Univ Sci Technol Med Sci.* 2013;33(1):86–89. PubMed:23392713. doi:10.1007/s11596-013-1076-0
39. Jin M, Wang J, Ji X, et al. MCUR1 facilitates epithelial-mesenchymal transition and metastasis via the mitochondrial calcium dependent ROS/Nrf2/Notch pathway in hepatocellular carcinoma. *J Exp Clin Cancer Res.* 2019;38(1):136. PubMed:30909929. doi:10.1186/s13046-019-1135-x
40. Lei C, Fan Y, Peng X, et al. P2Y11R regulates cytotoxicity of HBV X protein (HBx) in human normal hepatocytes. *Am J Transl Res.* 2019;11(5):2765–2774. PubMed:31217852.
41. Xie H, Xie D, Zhang J, et al. ROS/NF-κB signaling pathway-mediated transcriptional activation of TRIM37 promotes HBV-associated hepatic fibrosis. *Mol Ther Nucleic Acids.* 2020;22:114–123. PubMed:32916597. doi:10.1016/j.omtn.2020.08.014
42. Balkwill F, Mantovani A. Inflammation and cancer: back to Virchow? *Lancet.* 2001;357(9255):539–545. PubMed:11229684. doi:10.1016/S0140-6736(00)04046-0
43. Kuroda T, Kitadai Y, Tanaka S, et al. Monocyte chemoattractant protein-1 transfection induces angiogenesis and tumorigenesis of gastric carcinoma in nude mice via macrophage recruitment. *Clin Cancer Res.* 2005;11(21):7629–7636. PubMed:16278381. doi:10.1158/1078-0432.CCR-05-0798
44. Li X, Yao W, Yuan Y, et al. Targeting of tumour-infiltrating macrophages via CCL2/CCR2 signalling as a therapeutic strategy against hepatocellular carcinoma. *Gut.* 2017;66(1):157–167. PubMed:26452628. doi:10.1136/gutjnl-2015-310514
45. Shih YT, Wang MC, Zhou J, et al. Endothelial progenitors promote hepatocarcinoma intrahepatic metastasis through monocyte chemotactic protein-1 induction of microRNA-21. *Gut.* 2015;64(7):1132–1147. PubMed:24939570. doi:10.1136/gutjnl-2013-306302
46. Liu X, Jing X, Cheng X, et al. FGFR3 promotes angiogenesis-dependent metastasis of hepatocellular carcinoma via facilitating MCP-1-mediated vascular formation. *Med Oncol.* 2016;33(5):46. PubMed:27044356. doi:10.1007/s12032-016-0761-9
47. Finotto S, Siebler J, Hausding M, et al. Severe hepatic injury in interleukin 18 (IL-18) transgenic mice: a key role for IL-18 in regulating hepatocyte apoptosis in vivo. *Gut.* 2004;53(3):392–400. PubMed:14960523. doi:10.1136/gut.2003.018572
48. Markowitz GJ, Yang P, Fu J, et al. Inflammation-dependent IL18 signaling restricts hepatocellular carcinoma growth by enhancing the accumulation and activity of tumor-infiltrating lymphocytes. *Cancer Res.* 2016;76(8):2394–2405. PubMed:26893476. doi:10.1158/0008-5472.CAN-15-1548
49. Osaki T, Péron JM, Cai Q, et al. IFN-gamma-inducing factor/IL-18 administration mediates IFN-gamma- and IL-12-independent antitumor effects. *J Immunol.* 1998;160(4):1742–1749. PubMed:9469432.
50. Zhang Y, Huang G, Miao H, et al. Apatinib treatment may improve survival outcomes of patients with hepatitis B virus-related sorafenib-resistant hepatocellular carcinoma. *Ther Adv Med Oncol.* 2020;12(1758835920937422):1758835920937422. PubMed:32754228. doi:10.1177/1758835920937422
51. Lin JX, Xu YC, Lin W, et al. Effectiveness and safety of apatinib plus chemotherapy as neoadjuvant treatment for locally advanced gastric cancer: a nonrandomized controlled trial. *JAMA Netw Open.* 2021;4(7):e2116240. PubMed:34241629. doi:10.1001/jamanetworkopen.2021.16240
52. Hu Z, Dong N, Lu D, et al. A positive feedback loop between ROS and Mx1-0 promotes hypoxia-induced VEGF expression in human hepatocellular carcinoma cells. *Cell Signal.* 2017;31:79–86. PubMed:28065785. doi:10.1016/j.cellsig.2017.01.007
53. Lin Y, Zhai E, Liao B, et al. Autocrine VEGF signaling promotes cell proliferation through a PLC-dependent pathway and modulates apatinib treatment efficacy in gastric cancer. *Oncotarget.* 2017;8(7):11990–12002. PubMed:28061477. doi:10.18632/oncotarget.14467